

Spontaneous in-plane anomalous Hall response observed in a ferromagnetic oxide

Shinichi Nishihaya,¹ Yuta Matsuki,¹ Haruto Kaminakamura,¹
Yoshiya Murakami,¹ Hiroaki Ishizuka,¹ Masaki Uchida^{1,*}

¹Department of Physics, Institute of Science Tokyo, Tokyo 152-8551, Japan

*To whom correspondence should be addressed: E-mail: m.uchida@phys.sci.isct.ac.jp

Recent observation of anomalous Hall effect (AHE) induced by magnetic field or spin magnetization lying in the Hall deflection plane has sparked interest in diverse mechanisms for inducing the Hall vector component perpendicular to the applied magnetic field. Such off-diagonal coupling, which is strictly constrained by symmetry of the system, provides new degrees of freedom for engineering Hall responses. However, spontaneous response as extensively studied for out-of-plane AHE remains unexplored. Here we elucidate in-plane AHE in a typical ferromagnetic oxide SrRuO₃. The (111)-orientated ultrathin films with in-plane easy axes of spin magnetization exhibit spontaneous AHE at zero field, which is intrinsically coupled to the in-plane spin magnetization and controllable via its direction. Systematic measurements by varying azimuthal and polar field angles further reveal complex Hall responses shaped by higher-order terms allowed by trigonal distortion of the films. Our findings highlight versatile and controllable in-plane Hall responses with out-of-plane orbital ferromagnetism.

Introduction

Manipulation of spin and orbital magnetization by magnetic field is fundamental to diverse magnetotransport phenomena in magnets. The primary effect of the magnetic field is the Zeeman-type coupling, where magnetic moments couple diagonally to the applied field [1]. Recently, on the other hand, observation of Hall responses under the field applied within the Hall deflection plane has been reported (Fig. 1A) [2, 3, 4, 5, 6, 7]. In contrast to the conventional Hall effect induced by the out-of-plane magnetic field [8, 9], in-plane field induced anomalous Hall effect (in-plane AHE) can be interpreted as generation of the Hall vector component perpendicular to the in-plane magnetic field. Namely, it is an off-diagonal response to the magnetic field.

Following the theoretical proposals of in-plane AHE and its quantization in topological materials [10, 11, 12, 13, 14, 15, 16, 17], experimental observations of in-plane AHE in various materials have invoked interest in detailed mechanisms for realizing such off-diagonal responses [2, 3, 4, 5, 6, 7]. Among them, the in-plane AHE observed for Weyl semimetals Fe_3Sn_2 [5] and EuCd_2Sb_2 [6], which exhibits three-fold symmetry for the in-plane field rotation, has been understood as a consequence of band structure and quantum geometry modulations induced by the in-plane magnetic field. The in-plane field induced modulations are of purely intrinsic origins and thus strictly follows the crystal symmetry [21, 22], exhibiting the unique field direction dependence (Fig. 1B). In particular, out-of-plane Weyl points shifting by the in-plane field corresponds to manifestation of orbital magnetization in the out-of-plane direction [18, 19, 20].

So far research on in-plane AHE has been limited to non-magnetic [2, 3, 4], antiferromagnetic [6] or soft-magnetic materials [5, 7] with negligible magnetic hysteresis. As shown in Fig. 1C, hard ferromagnets potentially host anomalous Hall conduction and out-of-plane orbital ferromagnetism at zero field. Such a spontaneous response involving the off-diagonal coupling between orbital and spin degrees of freedom provides new opportunities for engineering the Hall transport. On the other hand, spin canting or reorientation derived by magnetocrystalline or shape magnetic anisotropy in ferromagnets may complicate observations by inducing the out-

of-plane spin magnetization component and conventional out-of-plane AHE. From this viewpoint, a ferromagnet with in-plane easy axes is highly desired for elucidating the pure response coupled to the in-plane spin magnetization.

Here, we study spontaneous in-plane AHE observed in films of ferromagnetic perovskite oxide SrRuO₃. The band structure of SrRuO₃ hosting several Weyl point pairs near the Fermi level [23, 24] is expected to be beneficial for realizing large in-plane AHE. (111)-oriented ultrathin SrRuO₃ films are epitaxially grown on the (111) SrTiO₃ substrate with threefold rotational symmetry about the out-of-plane direction (see Supplementary Note S1 for structural characterization). A giant in-plane AHE comparable to the out-of-plane AHE is observed in the SrRuO₃ ultrathin films, where the anomalous Hall conduction persists at zero field and can be controlled via the in-plane spin magnetization direction. Detailed measurements by varying azimuthal and polar angles of the field confirm that the SrRuO₃ ultrathin films possess in-plane easy axes, and reveal that the observed in-plane AHE is an off-diagonal response intrinsically coupled to the in-plane spin magnetization through higher-order terms allowed by trigonal distortion of the films.

Results

Out-of-plane and in-plane AHE

Figure 2A shows conventional Hall resistivity ρ_{yx} measured for a (111) SrRuO₃ film with thickness of 4.1 nm (sample A) with sweeping the out-of-plane magnetic field at 2 K. The Curie temperature T_C of this sample is determined to be 130 K, which is slightly lower than the bulk value but consistent with previous studies on (111) SrRuO₃ thin films (see Supplementary Note S2 for other fundamental transport) [26, 27, 28]. ρ_{yx} shows a large hysteresis loop characteristic to hard ferromagnets, also in good agreement with the previous studies [26, 27, 28]. The slope above the coercive field is roughly $0.03 \mu\Omega\text{cm}/\text{T}$.

AHE has not been fully examined in ferromagnets with in-plane spin magnetization. As shown in Fig. 2B, however, ρ_{yx} taken with sweeping the in-plane $[11\bar{2}]$ field at $\varphi = 0^\circ$ exhibits

significantly large values comparable to the out-of-plane scan, and continues to increase above the coercive field with a similar slope of $0.03 \mu\Omega\text{cm}/\text{T}$. Moreover, ρ_{yx} in the in-plane scan also remains finite at zero magnetic field accompanied with large hysteresis. Importantly, the present SrRuO₃ ultrathin films possess in-plane easy axes as shown later with the field angle dependence, and the observed AHE cannot be explained by out-of-plane canting of spin magnetization. The observation rather highlights the importance of out-of-plane orbital magnetization coupled to the in-plane spin magnetization.

ρ_{yx} taken at $\varphi = 60^\circ$ shows similar in-plane field dependence with signs opposite to the $\varphi = 0^\circ$ case. These observations are also consistent with symmetry of the trigonally distorted (111) SrRuO₃ thin films, which have a C_3 axis along the [111] direction, C_2 axes along the $[1\bar{1}0]$ and its equivalent directions, and mirror planes on the $(1\bar{1}0)$ and its equivalent planes. This allows the emergence of finite in-plane AHE with opposite signs centered at $\varphi = 0^\circ, 120^\circ, 240^\circ$ and $\varphi = 60^\circ, 180^\circ, 300^\circ$ [21, 22].

Azimuthal angle dependence

Figure 3A demonstrates φ dependence of ρ_{yx} , taken with rotating the in-plane magnetic field on the (111) plane for sample A. $\rho_{yx}(\varphi)$ is derived by antisymmetrization of the raw data $\rho_{yx,\text{raw}}$, as expressed by $\rho_{yx}(\varphi) = (\rho_{yx,\text{raw}}(\varphi) - \rho_{yx,\text{raw}}(\varphi + 180^\circ))/2$. When the field is above the in-plane coercive field of about 3 T, $\rho_{yx}(\varphi)$ exhibits a sinusoidal curve with three-fold symmetry, which is similar to the in-plane AHE reported for antiferromagnets and soft ferromagnets [5, 6, 7]. Its magnitudes and signs at $\varphi = 0^\circ$ and 60° are also consistent with the in-plane field scan data.

To investigate φ dependence of the Hall resistivity at zero field $\rho_{yx,0\text{T}}$, we repeatedly performed a procedure at each φ , which involves increasing the in-plane field to 9 T, returning it to 0 T, and then measuring the Hall resistivity. Here $\rho_{yx,0\text{T}}(\varphi)$ is obtained by antisymmetrization of a pair of raw data $\rho_{yx,0\text{T},\text{raw}}(\varphi)$ and $\rho_{yx,0\text{T},\text{raw}}(\varphi + 180^\circ)$. As shown in Fig. 3B, $\rho_{yx,0\text{T}}$ exhibits a rather square-wave curve with three-fold symmetry for rotation of the polarizing field, taking values consistent with the field scans at $\varphi = 0^\circ$ and 60° in Fig. 2B. $\rho_{yx,0\text{T}}$ decreases with

increase in temperature and disappears at T_C , confirming that this response is indeed related to the ferromagnetic ordering in SrRuO₃ (see Supplementary Note S3 for its detailed temperature dependence). Similar square-wave curves are reproducibly confirmed in $\rho_{yx,0T}$ taken for another (111) SrRuO₃ film with thickness of 7.0 nm (sample B) shown in Fig. 3C, regardless of the current direction on the plane. Difference of the φ dependence between the sinusoidal wave at 9 T and the square-like wave at 0 T suggests the presence of magnetic anisotropy with in-plane easy axes pointing to the $[11\bar{2}]$ and its equivalent directions.

Polar angle dependence

To further clarify the magnetic anisotropy near zero field, we present θ dependence of $\rho_{yx,0T}$ measured on the $(\bar{1}10)$ or $\varphi = 0^\circ$ plane in Fig. 4A. Here $\rho_{yx,0T}(\theta)$ is derived by antisymmetrization of $\rho_{yx,0T,raw}(\theta)$ and $\rho_{yx,0T,raw}(\theta + 180^\circ)$. $\rho_{yx,0T}(\theta)$ exhibits a plateau structure not only around the out-of-plane $[111]$ and $[\bar{1}\bar{1}\bar{1}]$ directions but also over the range including the in-plane $[11\bar{2}]$ direction. In addition, the θ scans taken at various magnetic fields (see Figure Supplementary Figure S4) reveal that $\rho_{yx}(\theta)$ exhibits a pronounced hysteresis loop around the $[00\bar{1}]$ and $[11\bar{1}]$ directions while the hysteresis loop is closed around the in-plane $[11\bar{2}]$ direction. All of these observations evidence that the SrRuO₃ ultrathin film possesses relatively strong in-plane shape magnetic anisotropy in addition to $\langle 111 \rangle$ magnetocrystalline anisotropy, realizing a ferromagnetic state with the spins aligned to the in-plane $[11\bar{2}]$ direction when the θ is close to 90° . Therefore, the observed spontaneous in-plane AHE is not due to out-of-plane canting of the spin magnetization, and it can be regarded as out-of-plane orbital ferromagnetism off-diagonally coupled to the in-plane spin magnetization.

Figure 4B presents θ scans measured at 9 T for the sweep from $[\bar{1}\bar{1}\bar{1}]$ toward $[111]$ and its reverse on the $\varphi = 0^\circ$ plane (See Supplementary Figure S5 for θ scans performed on the $\varphi = 60^\circ$ plane). Figure 4C compares θ scans measured at various magnetic fields for a forward sweep from $[\bar{1}\bar{1}\bar{1}]$ to $[111]$ (see also Supplementary Figures S4 for both the sweeps at various fields). While the effect of in-plane magnetic anisotropy is pronounced at the low fields, $\rho_{yx}(\theta)$ measured at high fields such as above 6 T exhibits negligibly small hysteresis, indicating that

the spin magnetization almost follows the applied field direction during the sweep. $\rho_{yx}(\theta)$ at high fields exhibits nonmonotonic dependence accompanied by local minimum and maximum around $[11\bar{1}]$ and $[00\bar{1}]$ directions, respectively. In particular, the local maximum around $[11\bar{1}]$ exhibiting a positive sign, which is opposite to the sign at $[111]$. This sign change feature strongly indicates the necessity of considering a higher-order effect due to magnetic field B [6] or magnetization M [7], which can be effectively regarded as generation of the out-of-plane orbital magnetization component by the in-plane field.

Discussion

As the Hall effect is a field-odd response, $B_i B_j B_k$ or $M_i M_j M_k$ with i, j, k Cartesian indices can be the leading term of the higher-order effect. By introducing the direction cosines α_i and β_i and unit vectors e_i along the principal axes, a general expansion of the Hall conductivity on the xy plane perpendicular to $\hat{z} = \beta_i e_i$ in cubic systems is expressed as

$$\sigma_{xy,\text{cubic}}(\mathbf{B}) = \sigma^{(1)} B \alpha_i \beta_i + \sigma^{(3)} B^3 \alpha_i^3 \beta_i + \sigma^{(5)} B^5 \alpha_i^5 \beta_i + \dots \quad (1)$$

or

$$\sigma_{xy,\text{cubic}}(\mathbf{M}) = \sigma^{(1)} M \alpha_i \beta_i + \sigma^{(3)} M^3 \alpha_i^3 \beta_i + \sigma^{(5)} M^5 \alpha_i^5 \beta_i + \dots \quad (2)$$

for magnetic field vector $\mathbf{B} = B \alpha_i e_i$ or magnetization vector $\mathbf{M} = M \alpha_i e_i$. By introducing anisotropy terms, the anomalous Hall conductivity outside the hysteresis loop can be expanded with respect to the magnetic field in the end. According to Eq. (1), ρ_{yx} on the (111) plane is usually dominated by the field-linear term proportional to $B_{[100]} + B_{[010]} + B_{[001]}$, or equivalently, to $B_{[111]}$; namely, ρ_{yx} changes proportionally with $B \cos \theta$, resulting in the absence of in-plane AHE. In cases with significant contributions from higher-order terms, on the other hand, ρ_{yx} manifests a characteristic θ dependence reflecting the crystal symmetry, while it appears always with three-fold rotational symmetry in the φ scan.

Figure 4D shows simulated θ dependence of the anomalous Hall conductivity σ_{xy} on the $\varphi = 0^\circ$ plane considering different higher-order terms. The third-order term in ρ_{yx} on the cubic

(111) plane is proportional to $B_{[100]}^3 + B_{[010]}^3 + B_{[001]}^3$, leading to a nonmonotonic θ dependence with a finite value at $\theta = 90^\circ$ (black curve in Fig. 4D). On the other hand, the experimentally observed behavior shown in Fig. 4B cannot be fitted well with the $B_{[100]}^3 + B_{[010]}^3 + B_{[001]}^3$ term. This suggests that it may be necessary to consider the effect of trigonal distortion which breaks the three-fold rotational symmetry about the $[\bar{1}11]$, $[1\bar{1}1]$, and $[11\bar{1}]$ directions (see Supplementary Note S1 for structural characterization). This allows other third-order terms such as $B_{[100]}B_{[010]}B_{[001]}$, which actually involves the local maximum of σ_{xy} at $[11\bar{1}]$ with a sign opposite to $[111]$ on the $\varphi = 0^\circ$ plane (red curve in Fig. 4D). From the same discussion, the spontaneous Hall response at zero field can be understood based on the higher order terms of the spin magnetization M .

In summary, we demonstrate spontaneous in-plane AHE in (111)-oriented ultrathin films of a hard ferromagnet SrRuO₃. Reflecting the crystal symmetry, the in-plane AHE emerges with three-fold symmetry for the field rotation on the Hall deflection plane. Off-diagonally coupled to the in-plane spin magnetization, the spontaneous anomalous Hall conduction and associated out-of-plane orbital magnetization persist even at zero field, and their sign can be switched via coupling to the in-plane spin magnetization. Moreover, the polar angle scans reveal the peculiar nonmonotonic behavior which suggests the contribution of the higher-order terms allowed under the trigonal distortion. While it is difficult to quantify the contribution from each term, our observations highlight the unique and spontaneous appearance of in-plane AHE reflecting the crystal symmetry, magnetic hysteresis, and magnetic anisotropy in the conventional ferromagnet. The present work broadens the horizons of Hall physics by demonstrating essential control of the Hall conduction by the in-plane magnetic field and its history.

Materials and Methods

Epitaxial film growth

(111)-oriented SrRuO₃ films were grown on (111) SrTiO₃ substrates in an Eiko EB-9000S oxide molecular beam epitaxy chamber equipped with a semiconductor-laser heating system

[29, 30]. SrTiO₃ substrates were annealed at 870 °C prior to the growth, and then SrRuO₃ films were grown at 650 °C by supplying 4N Sr from a conventional Knudsen cell, 3N5 Ru from an electron beam evaporator, and O₃ (60%) + O₂ (40%) from a Meidensya MPOG-RDE01C ozone generator. The film thickness was typically designed at about 4 nm.

Magnetotransport measurements

Longitudinal resistivity ρ_{xx} and Hall resistivity ρ_{yx} on Hall bar devices were measured using the conventional low-frequency lock-in technique. Field angle dependences of ρ_{xx} and ρ_{yx} up to 9 T were measured using a sample rotator in a Cryomagnetics cryostat system equipped with a superconducting magnet. The magnetotransport measurements were performed with changing the magnetic field direction within the (111) plane with an azimuthal angle φ (measured from $[11\bar{2}]$), and also from the out-of-plane $[111]$ direction toward an in-plane one with a polar angle θ (measured from $[111]$).

References and Notes

- [1] J. J. Sakurai, *Modern Quantum Mechanics* (Benjamin/Cummings, Menlo Park, CA, 1985).
- [2] T. Liang, J. Lin, Q. Gibson, S. Kushwaha, M. Liu, W. Wang, H. Xiong, J. A. Sobota, M. Hashimoto, P. S. Kirchmann, Z.-X. Shen, R. J. Cava, and N. P. Ong, Anomalous Hall effect in ZrTe₅. *Nat. Phys.* **14**, 451–455 (2018).
- [3] J. Zhou, W. Zhang, Y.-C. Lin, J. Cao, Y. Zhou, W. Jiang, H. Du, B. Tang, J. Shi, B. Jiang, X. Cao, B. Li, Q. Fu, C. Zhu, W. Guo, Y. Huang, Y. Yao, S. S. P. Parkin, J. Zhou, Y. Gao, Y. Wang, Ya. Hou, Y. Yao, K. Suenaga, X. Wu, and Z. Liu, Heterodimensional superlattice with in-plane anomalous Hall effect. *Nature* **609**, 46–51 (2022).
- [4] E. Lesne, Y. G. Sağlam, R. Battilomo, M. T. Mercaldo, T. C. v. Thiel, U. Filippozzi, C. Noce, M. Cuoco, G. A. Steele, C. Ortix, and A. D. Caviglia, Designing spin and orbital sources of Berry curvature at oxide interfaces. *Nat. Mater.* **22**, 576 (2023).

- [5] L. Wang, J. Zhu, H. Chen, H. Wang, J. Liu, Y.-X. Huang, B. Jiang, J. Zhao, H. Shi, G. Tian, H. Wang, Y. Yao, D. Yu, Z. Wang, C. Xiao, S. A. Yang, and X. Wu, Orbital Magneto-Nonlinear Anomalous Hall Effect in Kagome Magnet Fe_3Sn_2 . *Phys. Rev. Lett.* **132**, 106601 (2024).
- [6] A. Nakamura, S. Nishihaya, H. Ishizuka, M. Kriener, Y. Watanabe, and M. Uchida, In-Plane Anomalous Hall Effect Associated with Orbital Magnetization: Measurements of Low-Carrier Density Films of a Magnetic Weyl Semimetal. *Phys. Rev. Lett.* **133**, 236602 (2024).
- [7] W. Peng, Z. Liu, H. Pan, P. Wang, Y. Chen, J. Zhang, X. Yu, J. Shen, M. Yang, Q. Niu, Y. Gao, D. Hou, Observation of the In-plane Anomalous Hall Effect induced by Octupole in Magnetization Space. arXiv:2402.15741 (2024).
- [8] E. H. Hall, On a New Action of the Magnet on Electric Currents. *Am. J. Math.* **2**, 287 (1879).
- [9] N. Nagaosa, J. Sinova, S. Onoda, A. H. MacDonald, and N. P. Ong, Anomalous Hall effect. *Rev. Mod. Phys.* **82**, 1539–1592 (2010).
- [10] X. Liu, H.-C. Hsu, and C.-X. Liu, In-plane Magnetization Induced Quantum Anomalous Hall Effect. *Phys. Rev. Lett.* **111**, 086802 (2013).
- [11] Y. Ren, J. Zeng, X. Deng, F. Yang, H. Pan, and Z. Qiao, Quantum anomalous Hall effect in atomic crystal layers from in-plane magnetization. *Phys. Rev. B* **94**, 085411 (2016).
- [12] J. Zhang, Z. Liu, and J. Wang, In-plane magnetic-field-induced quantum anomalous Hall plateau transition. *Phys. Rev. B* **100**, 165117 (2019).
- [13] S. Sun, H. Weng, and X. Dai, Possible quantization and half-quantization in the anomalous Hall effect caused by in-plane magnetic field. *Phys. Rev. B* **106**, L241105 (2022).

- [14] Z. Li, Y. Han, and Z. Qiao, Chern Number Tunable Quantum Anomalous Hall Effect in Monolayer Transitional Metal Oxides via Manipulating Magnetization Orientation. *Phys. Rev. Lett.* **129**, 036801 (2022).
- [15] L. Li, J. Cao, C. Cui, Z.-M. Yu, and Y. Yao, Planar Hall effect in topological Weyl and nodal line semimetals. *Phys. Rev. B* **108**, 085120 (2023).
- [16] J. Cao, W. Jiang, X.-P. Li, D. Tu, J. Zhou, J. Zhou, and Y. Yao, In-Plane Anomalous Hall Effect in \mathcal{PT} -Symmetric Antiferromagnetic Materials. *Phys. Rev. Lett.* **130**, 166702 (2023).
- [17] H. Wang, Y.-X. Huang, H. Liu, X. Feng, J. Zhu, W. Wu, C. Xiao, and S. A. Yang, Orbital Origin of the Intrinsic Planar Hall Effect. *Phys. Rev. Lett.* **132**, 056301 (2024).
- [18] P. Streda, Theory of quantised Hall conductivity in two dimensions. *J. Phys. C: Solid State Phys.* **15**, L717 (1982).
- [19] D. Xiao, M.-C. Chang, and Q. Niu, Berry phase effects on electronic properties. *Rev. Mod. Phys.* **82**, 1959 (2010).
- [20] N. Ito and K. Nomura, Anomalous Hall Effect and Spontaneous Orbital Magnetization in Antiferromagnetic Weyl Metal. *J. Phys. Soc. Jpn.* **86**, 063703 (2017).
- [21] T. Kurumaji, Symmetry-based requirement for the measurement of electrical and thermal Hall conductivity under an in-plane magnetic field. *Phys. Rev. Research* **5**, 023138 (2023).
- [22] J. Cao, W. Jiang, X.-P. Li, D. Tu, J. Zhou, J. Zhou, and Y. Yao, In-plane anomalous Hall effect in \mathcal{PT} -symmetric antiferromagnetic materials. *Phys. Rev. Lett.* **130**, 166702 (2023).

- [23] Z. Fang, N. Nagaosa, K. S. Takahashi, A. Asamitsu, R. Mathieu, T. Ogasawara, H. Yamada, M. Kawasaki, Y. Tokura, and K. Terakura, The Anomalous Hall Effect and Magnetic Monopoles in Momentum Space. *Science* **3**, 92-95 (2003).
- [24] S. Itoh, Y. Endoh, T. Yokoo, S. Ibuka, J.-G. Park, Y. Kaneko, K. S. Takahashi, Y. Tokura, and N. Nagaosa, Weyl fermions and spin dynamics of metallic ferromagnet SrRuO₃. *Nat. Commun.* **7**, 11788 (2016).
- [25] U. Kar, E. C.-H. Lu, A. Kr. Singh, P. V. Sreenivasa Reddy, Y. Han, X. Li, C.-T. Cheng, S. Yang, C.-Y. Lin, I.-C. Cheng, C.-H. Hsu, D. Hsieh, W.-C. Lee, G.-Y. Guo, and W.-L. Lee, Nonlinear and Nonreciprocal Transport Effects in Untwinned Thin Films of Ferromagnetic Weyl Metal SrRuO₃. *Phys. Rev. X* **14**, 011022 (2024).
- [26] W. Lin, L. Liu, Q. Liu, L. Li, X. Shu, C. Li, Q. Xie, P. Jiang, X. Zheng, R. Guo, Z. Lim, S. Zeng, G. Zhou, H. Wang, J. Zhou, P. Yang, Ariando, S. J. Pennycook, X. Xu, Z. Zhong, Z. Wang, and J. Chen, Electric Field Control of the Magnetic Weyl Fermion in an Epitaxial SrRuO₃ (111) Thin Film. *Adv. Mater.* **33**, 2101316 (2021).
- [27] H. Ryu, Y. Ishida, B. Kim, J. R. Kim, W. J. Kim, Y. Kohama, S. Imajo, Z. Yang, W. Kyung, S. Hahn, B. Sohn, I. Song, M. Kim, S. Huh, J. Jung, D. Kim, T. W. Noh, S. Das, and C. Kim, Electronic band structure of (111) SrRuO₃ thin film – an angle-resolved photoemission spectroscopy study. *Phys. Rev. B* **102**, 041102(R) (2020).
- [28] A. Rastogi, M. Brahlek, J. M. Ok, Z. Liao, C. Sohn, S. Feldman, and H. N. Lee Metal-insulator transition in (111) SrRuO₃ ultrathin films. *APL Mater.* **7**, 091106 (2019).
- [29] Y. Matsuki, S. Nishihaya, M. Kriener, R. Oshima, F. Miwa, and M. Uchida, Unconventional two-dimensional quantum oscillations in three-dimensional thick SrRuO₃ films. *Appl. Phys. Lett.* **125**, 113105 (2024).

- [30] R. Oshima, T. Hatanaka, S. Nishihaya, T. Nomoto, M. Kriener, T. C. Fujita, M. Kawasaki, R. Arita, and M. Uchida, Ferromagnetic state with large magnetic moments realized in epitaxially strained $\text{Sr}_3\text{Ru}_2\text{O}_7$ films. *Phys. Rev. B* **109**, L121113 (2024).

Acknowledgments

Funding: This work was supported by JST FOREST Program Grant Number JPMJFR202N and PRESTO Program Grant Number JPMJPR2452, by JSPS KAKENHI Grant Numbers JP22K18967, JP22K20353, JP23K13666, JP23K03275, JP24H01614, and JP24H01654 from MEXT, Japan, by Murata Science and Education Foundation, Japan, and by STAR Award funded by the Tokyo Tech Fund, Japan. **Author contributions:** M.U. conceived the project and designed the experiments. Y.Ma. and H.K. grew films and performed transport measurements with S.N. and Y.Mu. Y.Ma., H.K., and S.N. analyzed the data and M.U. and S.N. wrote the manuscript with input from all authors. H.I. jointly discussed the results. All authors have approved the final version of the manuscript. **Competing interests:** The authors declare that they have no competing interests. **Data and materials availability:** All data needed to evaluate the conclusions in the paper are present in the paper and/or the Supplementary Materials.

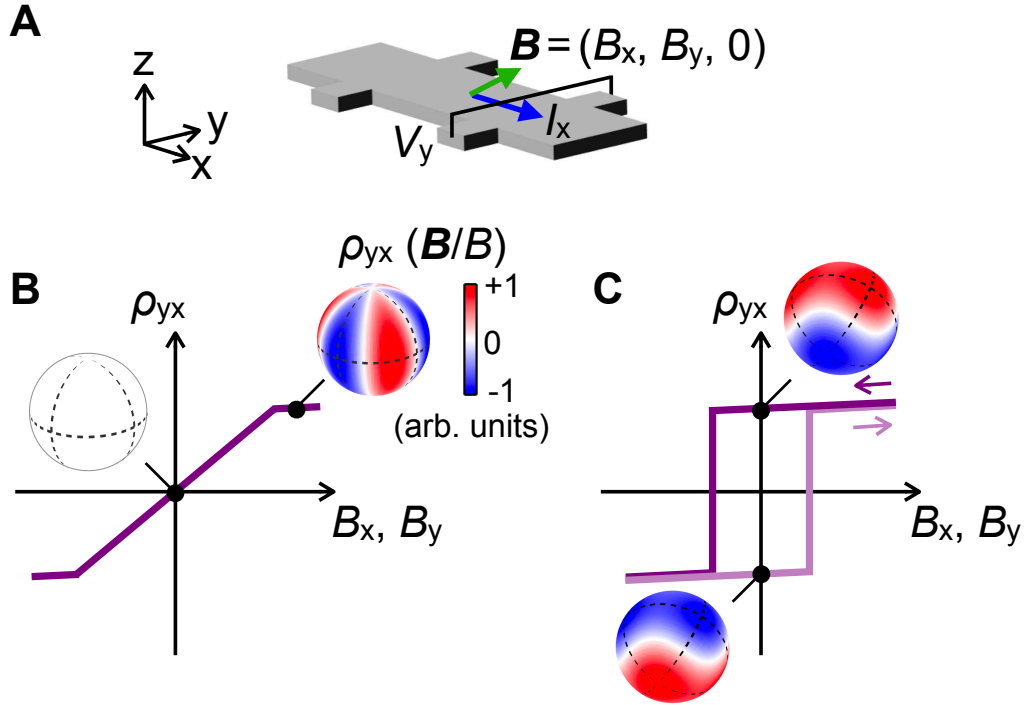


Fig. 1. Anomalous Hall effect by in-plane magnetic field. (A) Measurement configuration of anomalous Hall effect (AHE) under the in-plane magnetic field. A voltage V_y transverse to an electric current I_x can be generated depending not only on the value but also on the history of the in-plane magnetic fields B_x and B_y . (B) For antiferromagnets, the Hall resistivity ρ_{yx} becomes zero at zero magnetic field, even in the case that large ρ_{yx} with three-fold rotational symmetry around the z direction is induced by the in-plane field. A case of (001)-oriented trigonal systems is shown as an example of the field direction dependence of ρ_{yx} . (C) In hard ferromagnets, it is expected that ρ_{yx} spontaneously emerges even after turning off the in-plane magnetic field. A case of (111)-oriented cubic systems is exemplified.

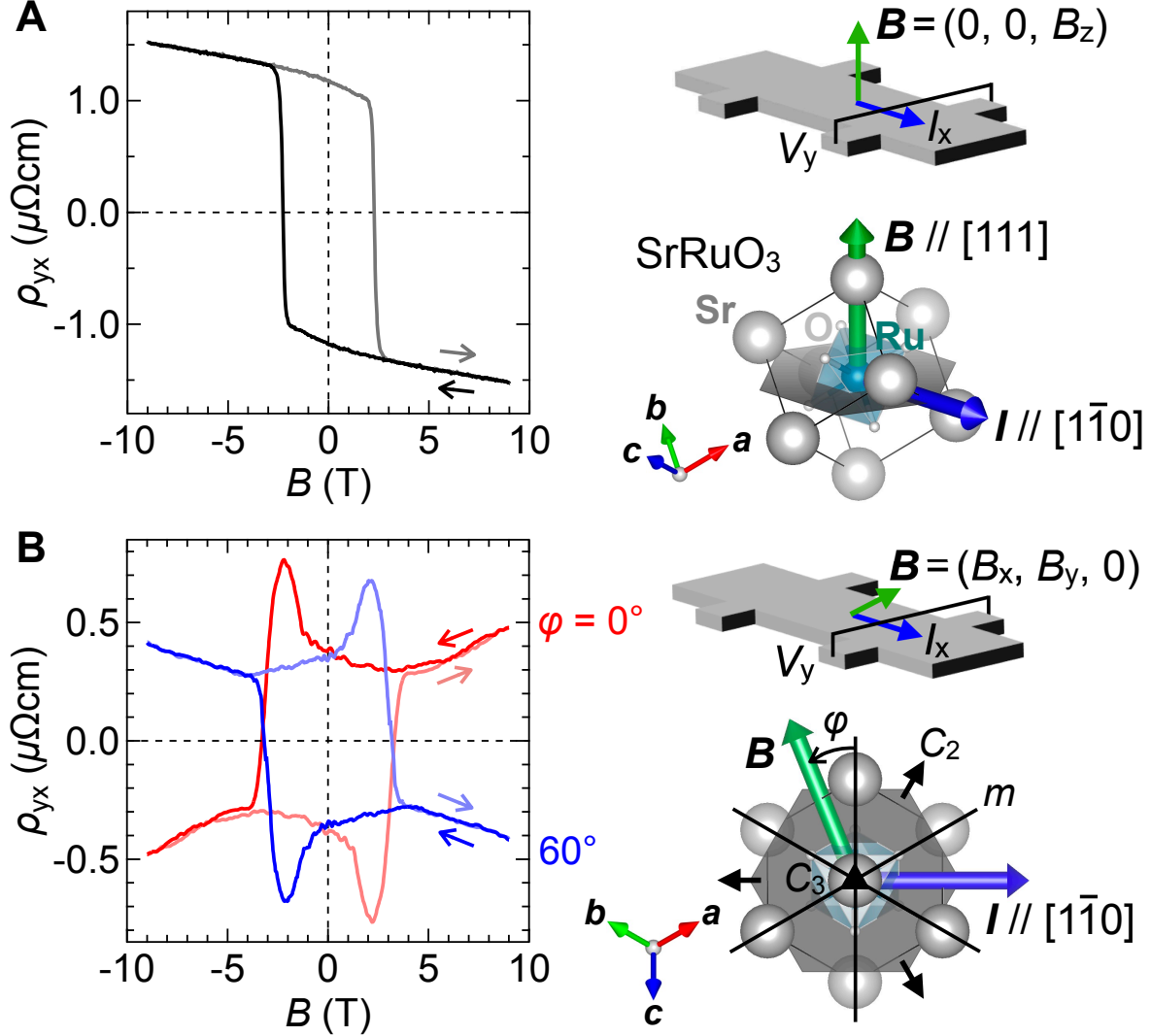


Fig. 2. Out-of-plane and in-plane AHE with a hysteresis loop. (A) Hall resistivity ρ_{yx} of a (111) SrRuO₃ film with thickness of 4.1 nm (sample A), taken with sweeping the out-of-plane magnetic field along the [111] direction at 2 K. Schematic illustration of the measurement configuration and its correspondence to the SrRuO₃ crystal structure are shown in the right panel. (B) ρ_{yx} measured with sweeping the in-plane field at azimuthal angles $\varphi = 0^\circ$ and 60° , where φ is measured from the $[11\bar{2}]$ direction. Illustration of the in-plane measurement configuration and its correspondence to the crystal structure are similarly shown, together with fundamental symmetry elements of the C_2 and C_3 rotation axes and the mirror planes.

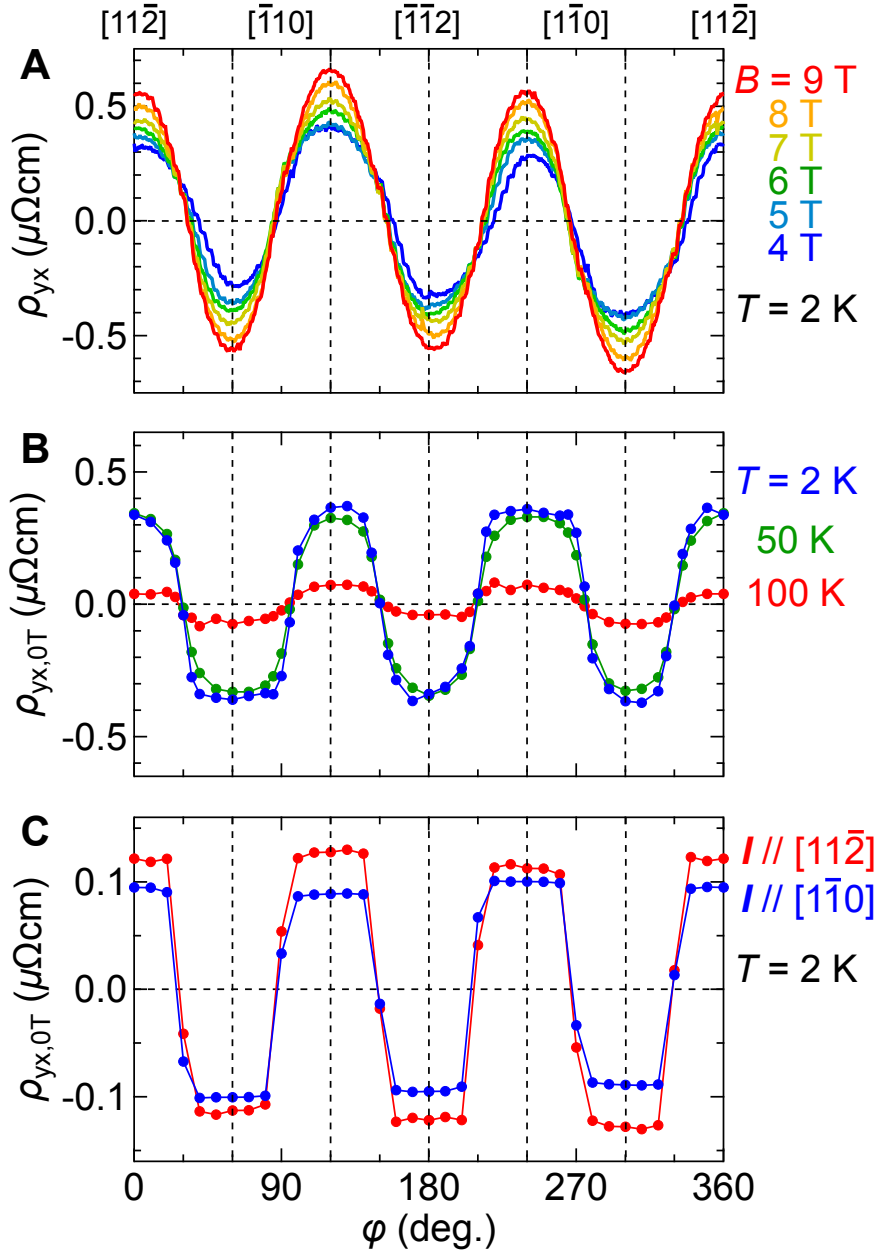


Fig. 3. In-plane AHE at zero magnetic field. (A) ρ_{yx} of the SrRuO₃ film (sample A), taken with continuously changing φ of various in-plane magnetic fields at 2 K. (B) Hall resistivity at zero magnetic field $\rho_{yx,0T}$, measured after applying the in-plane field of 9 T and then lowering it to 0 T at each φ . The measurements were performed at 2, 50, and 100 K. (C) $\rho_{yx,0T}$ measured for another (111) SrRuO₃ film with thickness of 7.0 nm (sample B) after the same magnetization process at 2 K. The measurements were performed on two Hall bar devices where the electric current flows along the $[1\bar{1}0]$ and $[11\bar{2}]$ directions, respectively.

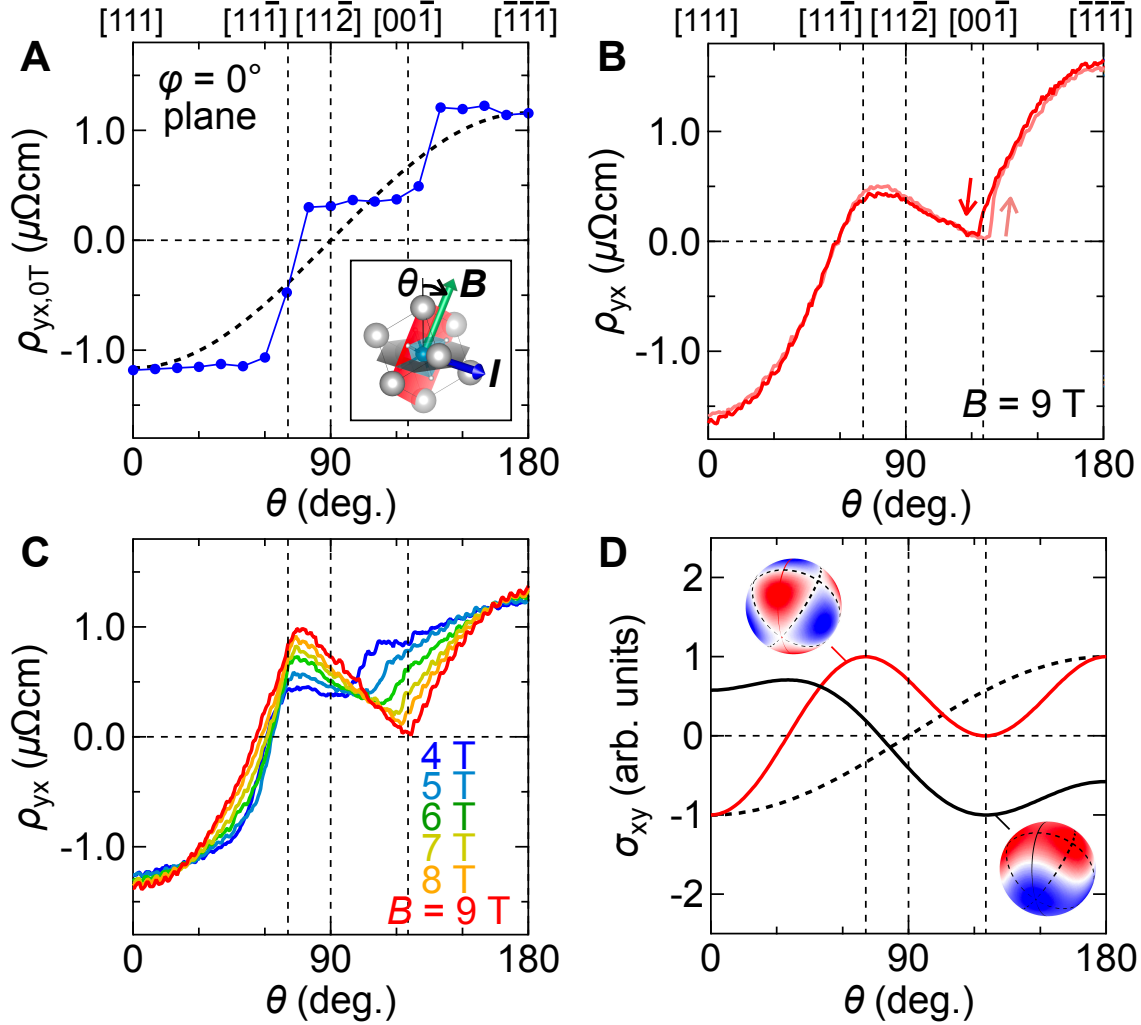


Fig. 4. Nonmonotonic polar angle dependence of AHE. (A) $\rho_{yx,0T}$ of the SrRuO_3 film (sample A), measured after applying the field of 9 T and then lowering it to 0 T at each polar angle θ on the $\varphi = 0^\circ$ plane at 2 K. θ is measured from the out-of-plane $[111]$ direction. (B) θ dependence of ρ_{yx} measured at 9 T for forward and reverse sweeps between $[111]$ and $[\bar{1}\bar{1}\bar{1}]$. (C) Comparison of $\rho_{yx}(\theta)$ measured at various magnetic fields. Only the forward sweeps from $[\bar{1}\bar{1}\bar{1}]$ to $[111]$ are shown. (D) Simulated θ dependence of the anomalous Hall conductivity σ_{xy} on the $\varphi = 0^\circ$ plane. Black and red solid curves represent σ_{xy} proportional to the $B_{[100]}^3 + B_{[010]}^3 + B_{[001]}^3$ and $B_{[100]}B_{[010]}B_{[001]}$ terms, respectively, while the conventional $B_{[100]} + B_{[010]} + B_{[001]}$ term is shown by a dashed curve.